https://doi.org/10.5194/acp-2019-1205
Preprint. Discussion started: 13 March 2020

Atmospheric Chemistry and Physics Discussions

Effective Radiative forcing from emissions of reactive gases and aerosols – a multimodel comparison

Gillian D. Thornhill[1], William J. Collins[1], Ryan J. Kramer[2], Dirk Olivié[3], Fiona O'Connor[4], Nathan L. Abraham[5], Susanne E. Bauer[6], Makoto Deushi[7], Louisa Emmons[8], Piers Forster[9], Larry Horowitz[10], Ben Johnson[4], James Keeble[5], Jean-Francois Lamarque[8], Martine Michou[11], Mike Mills[8], Jane Mulcahy[4], Gunnar Myhre[12], Pierre Nabat[11], Vaishali Naik[10], Naga Oshima[7], Michael Schulz[3], Chris Smith[9], Toshihiko Takemura[13], Simone Tilmes[8], Tongwen Wu[14], Guang Zeng[15], Jie Zhang[14].

[1]Department of Meteorology, University of Reading, Reading, RG6 6BB, UK
[2]Climate and Radiation Laboratory, NASA Goddard Space Flight Center, Greenbelt, MD 20771,USA, and Universities Space Research Association, 7178 Columbia Gateway Drive, Columbia, MD 21046, USA
[3]Norwegian Meteorological Institute, Oslo, Norway
[4] Met Office, Exeter, UK
[5]Department of Chemistry, University of Cambridge, Lensfield Road, Cambridge, CB2 1EW, U.K., National Centre for Atmospheric Science, U.K
[6] NASA Goddard Institute for Space Studies, USA
[7] Department of Atmosphere, Ocean and Earth System Modeling Research, Meteorological Research Institute, Japan
[8] National Centre for Atmospheric Research, Boulder, CO, USA
[9] University of Leeds, Leeds, UK
[10] GFDL/NOAA, Princeton University, Princeton, NJ 08540-6649
[11] Centre National de Recherches Météorologiques, Meteo-France, Toulouse Cedex, France
[12] CICERO – Centre for International Climate and Environmental Research Oslo, Oslo, Norway
[13] Research Institute for Applied Mechanics, Kyushu University, Japan
[14] Climate System Modeling Division, Beijing Climate Center, Beijing, China
[15] NIWA, Wellington, New Zealand

Correspondence to: Gillian D. Thornhill (g.thornhill@reading.ac.uk)

Abstract

This paper quantifies the effective radiative forcing from CMIP6 models of the present-day anthropogenic emissions of NOX, CO, VOCs, SO2, NH3, black carbon and primary organic carbon. Effective radiative forcing from pre-industrial to present-day changes in the concentrations of methane, N2O and halocarbons are quantified and attributed to their anthropogenic emissions.

https://doi.org/10.5194/acp-2019-1205
Preprint. Discussion started: 13 March 2020

Emissions of reactive species can cause multiple changes in the composition of radiatively active species: tropospheric ozone, stratospheric ozone, secondary inorganic and organic aerosol and methane. We therefore break down the ERFs from each emitted species into the contributions from the composition changes.
The 1850 to 2014 mean ERFs are -1.02 +/- 0.15 Wm^{-2} for SO2, -0.27 +/- 0.04 Wm^{-2} for organic carbon (OC), and 0.14 +/- 0.08 Wm^{-2} for black carbon (BC), and for the aerosols combined it is -0.94 +/- 0.08 Wm^{-2}. The means for the reactive gases are 0.70 +/- 0.08 Wm^{-2} for methane (CH4), 0.05 +/- 0.06 Wm^{-2} for NOx, -0.06 +/- 0.09 Wm^{-2} for volatile organic carbons (VOC), 0.17 +/- 0.04 Wm^{-2} for ozone (O3), 0.23 +/-0.03 Wm^{-2} for nitrous oxide (N2O) and -0.04 +/- 0.1 Wm^{-2} for hydrocarbon (HC). Differences in ERFs calculated for the different models reflect differences in the complexity of their aerosol and chemistry schemes, especially in the case of methane where tropospheric chemistry captures increased forcing from ozone production.

1. Introduction

The characterisation of the responses of the atmosphere, climate, and earth systems generally is essential for understanding, and countering, the impacts of climate change. As part of this effort there have been several projects directed at using climate models from different groups around the world to produce a systematic comparison of the simulations from these models, via the Coupled Model Intercomparison Project (CMIP), which is now in its 6th iteration (Eyring et al., 2016). This CMIP work has been subdivided into different areas of interest for addressing specific questions about climate, such as the impact of aerosols such as sulfates, black carbon (BC), organic carbon (OC), as well as other species which react in the atmosphere, e.g. methane, hydrocarbons, ozone and nitrous oxide, and the AerChemMIP (Collins et al., 2017) project is designed to examine the specific effects of these factors on the climate.
The focus of this work is to characterise the effect of the aerosols and chemically-reactive species on the radiation budget of the planet, referred to as radiative forcing, as an initial step to understanding the response of the atmosphere and earth system to changes in these components, whether those changes are due directly to anthropogenic emissions or to natural emissions responding to climate change (e.g. sea salt and dust which may change their emissions as a response to changes in wind speed, ocean temperature etc). In previous reports of the Intergovernmental Panel on Climate Change (IPCC) the effect of the various forcing agents on the radiation balance has been investigated in terms of the radiative forcing, (RF), which is a measure of how the radiative fluxes at the top of atmosphere (TOA) change in response to changes in e.g. emissions of CO2 or aerosols. There have been several definitions of radiative forcing, (Forster et al., 2016;Sherwood et al., 2015), which generally considered the instantaneous radiative forcing (IRF), or a combination of the IRF including the adjustment of the stratospheric temperature to the driver, generally termed the stratospherically-adjusted radiative forcing. More recently (Boucher, 2013;Chung and Soden, 2015) there has been a move towards using the effective radiative forcing (ERF) as the preferred metric, as this includes the rapid adjustments of the atmosphere to the perturbation, e.g. changes in cloud cover or type, water vapour, tropospheric temperature, which may affect the overall radiative balance of the atmosphere. In this work, this ERF is calculated using two atmospheric model simulations both with prescribed ocean conditions, but one having the perturbation we are interested in investigating, e.g. a change in emissions of aerosols. The difference in the net TOA flux between these two simulations is then defined as the ERF for that perturbation.

https://doi.org/10.5194/acp-2019-1205
Preprint. Discussion started: 13 March 2020

Previous efforts to understand the radiative forcing due to aerosols and chemistry have resulted in a wide spread of values from the different climate models, in part due to a lack of suitable model simulations for extracting the ERF from e.g. a specific change to an aerosol species. The experiments in the AerChemMIP project have been designed to address this in part, by defining consistent model set-ups to be used to calculate the ERFs, although the individual models will still have their own aerosol and chemistry modules, with varying levels of complexity and different approaches.

There are complexities in assessing how a particular forcing agent affects the climate system due to the interactions between some of the reactive gases; for example methane and ozone are linked in complex ways, and this increases the problem of understanding the specific contribution of each to the overall ERF when one of them is perturbed. An attempt to understand some of these interactions is discussed in Section 3.3 below.

The experimental set-up and models used are described in Section 2, the results for the aerosol and chemistry experiments are described in Section 3, and the results are discussed in section 4. Final conclusions are drawn in Section 5.

2. Experimental Setup

2.1 Models

This analysis is based on models participating in the Coupled Model Intercomparison Project (CMIP6) (Eyring et al., 2016), which oversees climate modelling efforts from a number of centres with a view to facilitating comparisons of the model results in a systematic framework. The overall CMIP6 project has a number of sub-projects, where those with interests in specific aspects of the climate can design and request specific experiments to be undertaken by the modelling groups. To understand the effects of aerosols and reactive chemistry on the climate a set of experiments was devised under the auspices of AerChemMIP (Collins et al., 2017), described in Section 2.2.

The emissions of the anthropogenic and reactive species for use in the models are given in (Hoesly et al., 2018) and van Marle et al. (2017) although models use their own (Eyring et al., 2016) natural emissions, while the well-mixed greenhouse gases (WMGHG) are specified as concentrations either at the surface or in the troposphere. Not all of the models include interactive aerosols, tropospheric chemistry and stratospheric chemistry, which is the ideal for the AerChemMIP experiments, but those models which do not include all these processes provide results for a subset of the experiments described in Section 2.2

The models included in this analysis are summarised in Table 1, with an overview of the model set-up, aerosol scheme and type of chemistry models used included. A more detailed table is available in the supplementary materials, Table S1.

The CNRM-ESM2-1 model (Séférian et al 2019, Michou et al. 2019) includes an interactive tropospheric aerosol scheme, and an interactive gaseous chemistry scheme down to a level of 560 hPa. The sulfate precursors evolve to SO4 using a simple dependence on latitude. The cloud droplet number concentration (CDNC) is depending on SO4, organic matter and sea-salt concentrations, so the cloud-albedo effect is represented, although other aerosol-cloud interactions are not.

The UKESM1 model (Sellar et al., 2020)is includes an interactive stratosphere-troposphere gas-phase chemistry scheme (Archibald et al., 2019) using the UK Chemistry and Aerosol (UKCA; (Morgenstern et al., 2009;O'Connor

https://doi.org/10.5194/acp-2019-1205
Preprint. Discussion started: 13 March 2020

et al., 2014) model. The UKCA aerosol scheme, called GLOMAP-mode, is a two-moment scheme for the simulation of tropospheric black carbon (BC), organic carbon (OC), SO4, and sea salt. Dust is modelled independently using the bin scheme of (Woodward, 2001). The UKCA chemistry and aerosol schemes are coupled such that the secondary aerosol (SO4, OA) formation rates depend on oxidants from the stratosphere-troposphere chemistry scheme (Archibald et al., 2019;Sellar et al., 2020), Mulcahy et al 2019, in prep). Aerosol particles are activated into cloud droplets using the activation scheme of (Abdul-Razzak and Ghan, 2000) which is dependent on aerosol size distribution, aerosol composition, and meteorological conditions. Changes in CDNC affect cloud droplet effective radius ((Jones et al., 2001) and the autoconversion of cloud liquid water in to rain water (Khairoutdinov and Kogan, 2000), which both influence cloud albedo ((Mulcahy et al., 2018); Mulcahy et al., 2019 in prep). Stratospheric aerosols (aerosol optical depth and surface area density) are prescribed in the model (Sellar et al., 2019b). A full description and evaluation of the chemistry and aerosol schemes in UKESM1 can be found in (Archibald et al., 2019) and Mulcahy et al. (2019), respectively.

The MIROC6 model includes the Spectral Radiation-Transport Model for Aerosol Species (SPRINTARS) aerosol model which predicts mass mixing ratios of the main tropospheric aerosols and models aerosol-cloud interactions in which aerosols alter cloud microphysical properties and affect the radiation budget by acting as cloud condensation and ice nuclei. The sulfate and carbonaceous aerosols are treated as externally mixed in this model. The CDNC and ice crystal number are used to calculate the aerosol indirect effect and cloud nucleation process (Takemura et al., 2005), (Watanabe et al., 2010), Takemura et al 2018). It also includes gas phase chemistry.

The MRI-ESM2 model (Yukimoto et al., 2019) has the MASINGAR mk-2 aerosol scheme, and a chemistry model, MRI-CCM2 ((Deushi and Shibata, 2011) which models chemistry processes for O3 and other trace gases from the surface to the stratosphere. The aerosol scheme includes aerosol-chemistry interactions, and aerosol-cloud interactions (Kawai et al., 2019)

The BCC-ESM1 model (Wu et al., 2019b), (Wu et al., 2019a) models major aerosol species including gas-phase chemical reactions, secondary aerosol formation, and aerosol-cloud interactions including indirect effects are represented. It uses the BCC-AGCM3-Chem atmospheric chemistry model based on MOZART2 (Horowitz et al., 2003) which does not include stratospheric chemistry, so concentrations of ozone, CH4, and N2O at the top two model levels are the zonally and monthly values derived from the CMIP6 data package.

The NorESM2 model contains interactive aerosols. The OsloAero6 aerosol module (Olivié et al., in prep.) which contains some slight updates since (Kirkevåg et al., 2018) describes the formation and evolution of BC, OM, sulfate, dust, sea-salt and SOA. There is a limited gas-phase chemistry describing the oxidation of the aerosol precursors DMS, SO2, isoprene, and monoterpenes. Oxidant fields of OH, HO2, NO3 and O3 are prescribed climatological fields. As there is no ozone chemistry in the model, prescribed monthly-varying ozone fields are used for the radiation.

The GFDL-ESM4 model consists of the GFDL AM4.1 atmosphere component (Horowitz et al in prep 2019, Dunne et al in prep 2019) which includes an interactive tropospheric and stratospheric gas-phase and aerosol chemistry scheme. The model includes 56 prognostic (transported) tracers and 36 diagnostic (non-transported) chemical tracers, with 43 photolysis reactions, 190 gas-phase kinetic reactions, and 15 heterogeneous reactions. The tropospheric chemistry includes reactions for the NO_x-HO_x-O_x-CO-CH_4 system and oxidation schemes for other non-methane volatile organic compounds. The stratospheric chemistry accounts for the major ozone loss cycles (O_x, HO_x, NO_x, ClO_x, and BrO_x) and heterogeneous reactions on liquid and solid stratospheric aerosols as

https://doi.org/10.5194/acp-2019-1205
Preprint. Discussion started: 13 March 2020

in Austin et al. (2013). The bulk aerosol scheme, including 18 transported aerosol tracers, is similar to that in AM4.0 (Zhao et al., 2018), with the following updates: (1) ammonium and nitrate aerosols are treated explicitly, with ISORROPIA (Fountoukis and Nenes, 2007) used to simulate the sulfate–nitrate–ammonia thermodynamic equilibrium; (2) oxidation of sulfur dioxide and dimethyl sulfide to produce sulfate aerosol is driven by the gas-phase oxidant concentrations (OH, H_2O_2, and O_3) and cloud pH simulated by the online chemistry scheme, and (3) the rate of aging of black and organic carbon aerosols from hydrophobic to hydrophilic forms varies with calculated concentrations of hydroxyl radical (OH).

The CESM2-WACCM model includes interactive chemistry and aerosols for the troposphere, stratosphere and lower thermosphere (Emmons et al., 2010); (Gettelman et al., 2019)). It simulates 228 compounds, including the MAM4 4-mode Modal Aerosol Model. This version of MAM4 is modified to allow for the simulation of stratospheric aerosols from volcanic eruptions (from their SO2 emissions) and oxidation of OCS (Mills et al., 2016). The representation of secondary organic aerosols follows the Volatility Basis Set approached (Tilmes et al., 2019).

The IPSLCM6A-LR model used for this analysis has prescribed aerosols which were pre-calculated from an atmosphere-only configuration and then prescribed as monthly climatologies. The O3 is prescribed from the CMIP6 official dataset. The IPSL model results presented here are only for the piClim-aer experiment, and don't include results for this model for the additional AerChemMIP experiments.

Table 1 Components used in the Earth system models (detailed Table is in Supplemental material, Table S1)

	Aerosols	Tropospheric chemistry	Stratospheric chemistry
IPSL-CM6A-LR	Prescribed	No	No
NorESM2-LM	Interactive	SOA and sulfate precursor chemistry	No
UKESM1-LL	Interactive Tropospheric. Prescribed stratospheric	Interactive	Interactive
CNRM-ESM2-1	Interactive	Chemical reactions down to 560 hPa	Interactive
MRI-ESM2	Interactive	Interactive	Interactive
MIROC6	Interactive	SOA and sulfate precursor chemistry	No
BCC-ESM1	Interactive	Interactive	No
GFDL-ESM4	Interactive	Interactive	Interactive
CESM2-WACCM	Interactive	Interactive	Interactive

https://doi.org/10.5194/acp-2019-1205
Preprint. Discussion started: 13 March 2020

2.2 Experiments

The AerChemMIP timeslice experiments (Table 2) are used to determine the present day (2014) ERFs for the changes in emissions or concentrations of reactive gases, and aerosols or their precursors (Collins et al., 2017). The ERFs are calculated by comparing the change in net TOA radiation fluxes between two runs with the same prescribed sea surface temperatures (SSTs) and sea ice, but with NTCFs (reactive gas and aerosol emissions, also referred to as SLCFs – short-lived climate forcers) or WMGHG (methane, nitrous oxide, halocarbon) concentrations perturbed. The control run uses set 1850 pre-industrial values for the aerosol precursors, CH4, N2O, ozone precursors and CFC/HCFC, either as emissions or concentrations ((Hoesly et al., 2018;van Marle et al., 2017;Meinshausen et al., 2017). Monthly varying prescribed SSTs and sea-ice are taken from an 1850 coupled pre-industrial simulation. Each experiment then perturbs the pre-industrial value by changing one (or more) of the species to the 2014 value, while keeping SSTs and sea-ice prescribed as in the pre-industrial control. The NTCFs are perturbed individually or in groups. This provides ERFs for the specific emission or concentration change, but also for all aerosol precursor or NTCFs combined (Collins et al., 2017). For models without interactive tropospheric chemistry "NTCF" and "aer" experiments are the same; in the case of NorESM2 for the NTCF experiments the model attempts to mimic the full chemistry by setting the oxidants and ozone to 2014 values. The WMGHG experiments include the effects on aerosol oxidation, tropospheric and stratospheric ozone, and stratospheric water vapour depending on the model complexity.

Thirty years of simulation are used to minimise internal variability (mainly from clouds) (Forster et al, 2016.).

Table 2 List of fixed SST ERF simulations. (NTCF in Collins et al 2017 is also referred to as 'SLCF' in other publications) and for the purposes of this study excludes methane.

Experiment ID	CH_4	N_2O	Aerosol Precursors	Ozone Precursors	CFC/ HCFC	Number of models
piClim-control	1850	1850	1850	1850	1850	9
*piClim-**NTCF***	1850	1850	**2014**	**2014**	1850	7
*piClim-**aer***	1850	1850	**2014**	1850	1850	8
*piClim-**BC***	1850	1850	1850 (non BC) **2014** (BC)	1850	1850	6
*piClim-**O3***	1850	1850	1850	**2014**	1850	4
*piClim-**CH4***	**2014**	1850	1850	1850	1850	7
*piClim-**N2O***	1850	**2014**	1850	1850	1850	4
*piClim-**HC***	1850	1850	1850	1850	**2014**	5
*piClim-**NOX***	1850	1850	1850	1850 (non NO_x) **2014** (NO_x)	1850	3
*piClim-**VOC***	1850	1850	1850	1850 (non CO/VOC) **2014** (CO/VOC)	1850	3
*piClim-**SO2***	1850	1850	1850 (non SO2) **2014** (SO2)	1850	1850	6
*piClim-**OC***	1850	1850	1850 (non OC)	1850	1850	6

https://doi.org/10.5194/acp-2019-1205
Preprint. Discussion started: 13 March 2020

			2014 (OC)			
*piClim-**NH3***	1850	1850	1850 (non NH3) **2014** (NH3)	1850	1850	0

3. Methods

In the following analysis we use several methods to analyse the ERF and the relative contributions from different aerosols, chemistry and processes to the overall ERF for the models and experiments described above, where the appropriate model diagnostics were available.

3.1.1 Calculation of ERF using fixed SSTs

The ERF is calculated from the experiments described above, where the sea surface temperatures and sea-ice are fixed to climatological values. Here the ERF is defined as the difference in the net TOA flux between the perturbed experiments and the piClim-control experiment (Sherwood et al., 2015), calculated as the global mean for the 30 years of the experimental run (where the models were run longer than 30 years, the last 30 years was used). This allows us to calculate the ERF for the individual species based on the changes to the emission or concentrations between the control and perturbed runs of the models. The assumption is that there is minimal contribution from the climate feedback when the ocean state is fixed, but the resultant ERF includes rapid adjustments to the forcing agent in the atmosphere (Forster et al., 2016).

3.1.2 Kernel Analysis

Where the relevant data are available, we use the radiative kernel method (Smith et al., 2018;Soden et al., 2008;Chung and Soden, 2015) to break down the ERF into the instantaneous radiative forcing (IRF) and individual rapid adjustments (designated by A) which are radiative responses to changes in atmospheric state variables that are not coupled to surface warming. In this approach, ERF is defined as:

$$\mathrm{ERF} = \mathrm{IRF} + A_T + A_{ts} + A_q + A_a + A_c + e \quad (1)$$

where A_T = atmospheric temp., A_{ts} = surface temp., A_q = water vapour, A_a = albedo, A_c = clouds, e = radiative kernel error. Individual rapid adjustments (A_x) are computed as:

$$A_x = \frac{\delta R}{\delta x} dx \quad (2)$$

where $\frac{\delta R}{\delta x}$ is the radiative kernel, a diagnostic tool typically computed with an offline version of a GCM radiative transfer model that is initialized with climatological base state data and dx is the climate response of atmospheric state variable x, diagnosed directly from each model. Cloud rapid adjustments (A_C) are estimated by diagnosing cloud radiative forcing from model flux diagnostics and correcting for cloud masking using the kernel-derived non-cloud adjustments and IRF, following common practice (e.g. (Soden et al., 2008;Smith et al., 2018)), whereby:

$$A_C = (ERF - ERF^{clr}) - (\mathrm{IRF} - IRF^{clr}) - \sum_{x=[T,ts,q,a]} (A_x - A_x^{clr}) \quad (3)$$

https://doi.org/10.5194/acp-2019-1205
Preprint. Discussion started: 13 March 2020

Clear-sky IRF (IRF^{clr}) is estimated as the difference between clear-sky ERF (ERF^{clr})and the sum of kernel-derived clear-sky rapid adjustments (A_x^{clr}). Since estimates of $A_c$are dependent on IRF, the same differencing method cannot be used to estimate IRF under all-sky conditions without special diagnostics (in particular the isccp diagnostics) not widely available in the AerChemMIP archive. Alternatively, all-sky IRF is computed by scaling $IRF^{clr}$by a constant to account for cloud masking (Soden, Held et al. 2008; Kramer et al. 2020).

Kernels are available from several sources, and for this analysis we used kernels from CESM, ((Pendergrass et al., 2018), GFDL (Soden et al., 2008), HadGEM3, (Smith and Kramer 2020, submitted), and ECHAM6 ((Block and Mauritsen, 2013) and took the mean from the four kernels for each model. Overall the individual kernels produced very similar results for each model, as reported in (Smith et al., 2018).

3.1.3. Calculation of ERF using aerosol-free radiative fluxes

To understand the contributions of various processes to the overall ERF we can attempt to separate the ERF that is due to direct radiative forcing from that due to the effects of aerosol-cloud interactions; aerosols act on clouds in a variety of complex ways, by heating the clouds to cause burn-off (semi-direct effect Ackerman et al 2000), and via microphysical effects (e.g. the number of condensation nuclei and the effective radii of the cloud droplets, referred to as the cloud albedo effect and the cloud lifetime effect (Twomey, 1974;Albrecht, 1989;Pincus and Baker, 1994). Following the method of Ghan (2013) the direct forcing due to aerosols alone can be found by calculating the radiative fluxes from the model simulation ignoring the scattering and absorption by the aerosol – referred to in the equations below with the subscript 'af'. The other effects of the aerosol on the atmosphere (i.e. cloud changes, stability changes, dynamics changes) will still be present, however. The direct radiative effect (ERFari) here is the direct radiative forcing from the aerosol based on the all-sky fluxes with the aerosol, subtracted from the all-sky fluxes without the aerosol. This is a measure of the radiative effects due only to the aerosol. The effects of the aerosol on cloud radiative forcing is then obtained by using the difference between the aerosol-free all-sky fluxes and the aerosol-free clear-sky fluxes, which isolates the cloud effects, where cloud changes due to the presence of the aerosol will be present, but the radiative effects of the aerosol itself are removed (see eqns 4-5). The final term is the ERF as calculated from fluxes with neither clouds nor aerosols (ERFcs,af), attributed to the effect of aerosols on the surface albedo by (Ghan, 2013).

ERFari = (ERF - ERFaf) (4)

ERFaci = ERFaf - ERFcsaf (5)

4. Results

4.1 Aerosols

4.1.1 ERF vs SARF

The results in Fig (1) show the ERF, the tropospheric adjustments, and the stratospheric adjusted radiative forcing (SARF). As described in section 3.1.1 the ERFs are diagnosed from the radiative fluxes in the fixed SST experiments, and the tropospheric adjustments A_trop from the sum of all adjustments in section 3.2.2 apart from the stratospheric temperature adjustment. The SARF is then determined from SARF = ERF – A_trop.

https://doi.org/10.5194/acp-2019-1205
Preprint. Discussion started: 13 March 2020

The SARF and rapid adjustments should total the overall ERF, and comparing the ERF as calculated from the model output with the sum of the SARF and A_trop gives a difference of less than 3%, and in general less than 1%, confirming that the total ERF is accounted for by the combination of SARF and A_trop.

For aerosols, (with little stratospheric-temperature adjustment) the SARF is approximately the direct IRF; using the kernel method described above it is important to note that the IRF calculated here accounts for the presence of the clouds but does not include cloud changes such as the Twomey effect.

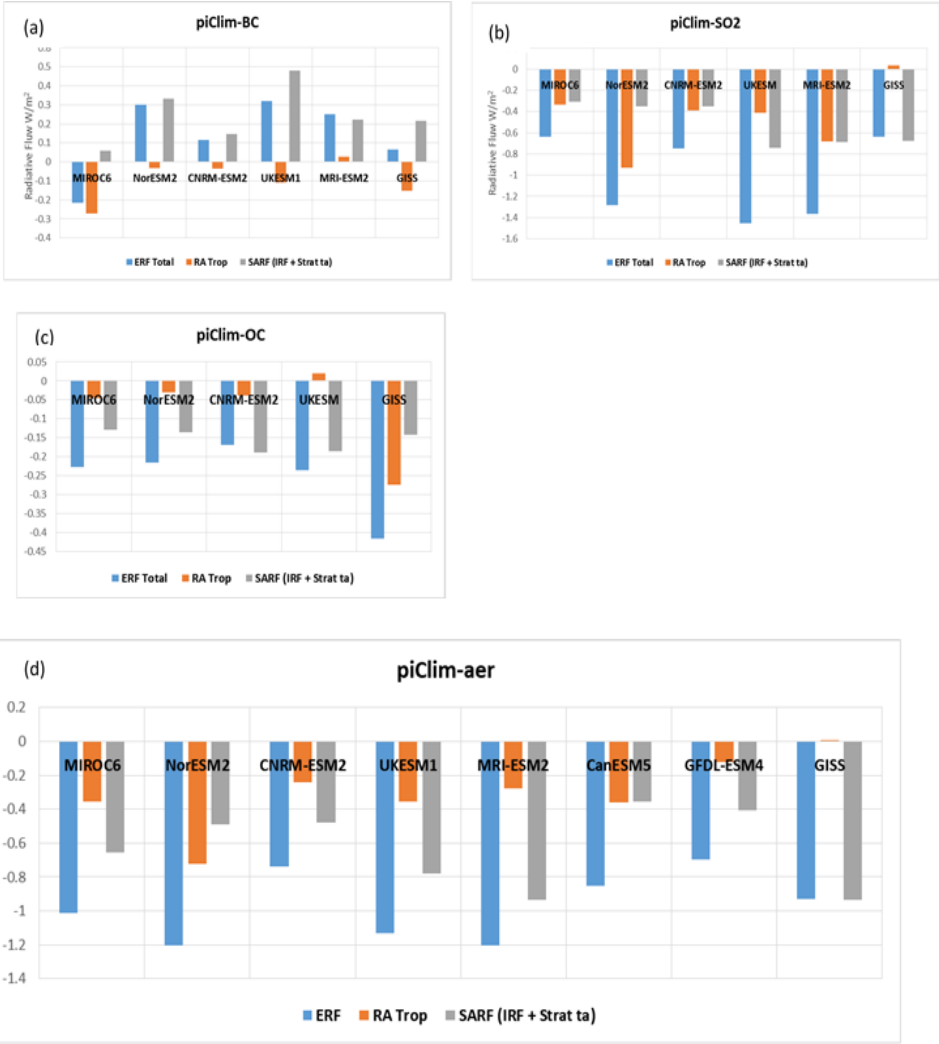

Fig. 1 Breakdown of the ERFs into the tropopause rapid adjustments and IRF (instantaneous radiative forcing) for aerosol species. (a) piClim-BC experiment, (b) piClim-SO2 experiment, (c) piClim-OC experiment, (d) piClim-aer experiment

The models show moderate agreement for the SARF for SO2 (range of -0.31 Wm^{-2} - 0.74 Wm^{-2}) and OC (-0.13 Wm^{-2} – 0.19 Wm^{-2}), with a much larger range for BC (0.06 Wm^{-2} to 0.48 Wm^{-2}). In MIROC6 the treatment of BC (Takemura & Suzuki 2019; Suzuki & Takemura 2019) leads to faster wet removal and hence lower SARF. Overall there is approximately a factor of 3 in the range of the SARF for total aerosols (-0.35 Wm^{-2} to -0.97 Wm^{-2}).

https://doi.org/10.5194/acp-2019-1205
Preprint. Discussion started: 13 March 2020

There are significant differences between the models in the A_trop for SO2; these vary by 0.04 Wm^{-2} to -0.93 Wm^{-2}, where the differences are dominated by the cloud adjustments (see Fig S3 for breakdowns of the rapid adjustments for all models) which here include the Twomey effect as part of the adjustment. The adjustments to BC are generally small with most models having a smaller positive adjustment to that reported by (Stjern et al., 2017;Samset et al., 2016;Smith et al., 2018) and others. The MRI-ESM2 model does have a slight positive adjustment, but it is small in magnitude but MIROC6 has a large negative adjustment which is large enough to lead to an overall negative ERF. We explore the adjustments to BC in more detail in the figure (2).

Examining the breakdown of the rapid adjustments for the piClim-BC experiments (Fig 2) we see considerable variability in the relative importance of the rapid adjustments; the cloud adjustment dominates in MIROC6, consistent with the increase in low clouds reported for this model in (Takemura & Suzuki 2019; Suzuki & Takemura 2019) causing a negative overall adjustment. The GISS model also has a large cloud rapid adjustment, but the larger positive value of the SARF leads to an overall positive ERF for this model. For UKESM1, CNRM-ESM2-1 and MRI-ESM2 a negative tropospheric temperature adjustment is balanced by the cloud and the water vapour adjustment, although the magnitude of the adjustments for MRI-ESM2 is at least twice that for the other two models.

The piClim-aer experiments show a broad consistency between the models, with the A_trop varying between 0.07 to -0.72 Wm^{-2}, where GISS has a slightly positive A_trop value. Overall the cloud rapid adjustments dominate for the piClim-aer experiments, with a contribution ranging from -0.77 Wm^{-2} to -0.22 Wm^{-2} (See fig S1).

The breakdown of the rapid adjustments for all the models are included in supplemental fig. S1, showing the contributions from each type of rapid adjustment for all the experiments for which we have the relevant diagnostics.

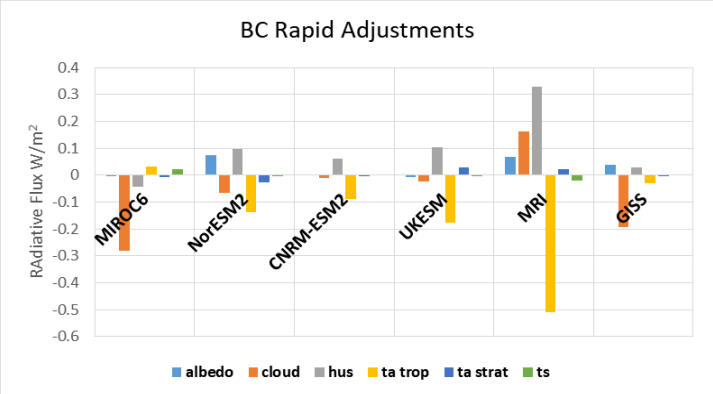

Fig. 2 Breakdown of the individual rapid adjustments for the piClim-BC experiments

4.1.2 Radiation and Cloud interactions

The second method of breaking down the ERF to constituents is described in Section 3.1.3, (the Gahn method), the results from which are shown in Table 3. Only four of the models under consideration have so far produced the necessary diagnostics for this calculation, and the results are presented in Table 3. For the experiments on

https://doi.org/10.5194/acp-2019-1205
Preprint. Discussion started: 13 March 2020

aerosols (aer, BC, SO2, OC) the ERFcs,af (the contribution due to the albedo changes from the aerosol) contribution is

Table 3 Results for ERFari, ERFaci and ERFcs,af for aerosol experiments from several models

	UKESM1			CNRM-ESM2			NorESM2			MRI-ESM2		
	ERFari	cs,af	ERFaci	ERFari	cs,af	ERFaci	ERFari	cs,af	ERFaci	ERFari	cs,af	ERFaci
aer	-0.16	0.05	-1.02	-0.21	0.08	-0.61	0.03	-0.03	-1.21	-0.32	0.09	-0.98
BC	0.38	0.00	-0.06	0.13	0.01	-0.03	0.35	0.07	-0.12	0.26	0.08	-0.09
OC	-0.15	-0.03	-0.09	-0.07	0.04	-0.14	-0.07	0.02	-0.16	-0.07	-0.05	-0.21
SO2	-0.48	0.02	-0.99	-0.29	0.08	-0.53	-0.19	-0.09	-1.01	-0.48	0.05	-0.93

small, and the ERF is largely a combination of the direct radiative effect, ERFari, and the cloud radiative effect, ERFaci. The ERFari is the direct effect of the aerosol due to scattering and absorption, and may be considered roughly equivalent to the rapid adjustments due to clouds (see Section 3.2.1).

For the BC experiment for CNRM-ESM2, MRI-ESM2 and UKESM1 the contribution of the cloud radiative effect is small, suggesting that the effects of the BC on the clouds through the semi-direct and indirect effects is minimal. The SO2 experiment shows a large cloud radiative effect, in fact the ERFaci is mostly double the ERFari in all the models, due to the large effect on clouds of SO2 and sulfates through the indirect and semi-direct effect. For the OC experiments the ERFaci is at least double the ERFari for all models.

Comparing the ERFari with the SARF calculated via the kernel analysis (Section 3.2.1) where the relevant model results are available, for the BC experiment we have reasonable agreement for all the models: UKESM1 (ERFari = 0.38Wm^{-2} and SARF = 0.48 Wm^{-2}), CNRM-ESM2 (ERFari = 0.13 Wm^{-2} and SARF = 0.15 Wm^{-2}), NorESM2 (ERFari = 0.35 Wm^{-2} and SARF = 0.33 Wm^{-2} and MRI-ESM2 (ERFari = 0.26 Wm^{-2} and SARF = 0.22 Wm^{-2} , although the values for NorESM are smaller than for the other 3 models. The results for the SO2 and OC experiments are less clear. In the case of SO2 the SARF is higher than the ERFari for NorESM2 (ERFari = -0.19 Wm^{-2}, SARF = -0.35 Wm^{-2}), for CNRM-ESM2 the ERFari is similar to the SARF value (ERFari = -0.29 Wm^{-2} and SARF = -0.35 Wm^{-2}), MRI-ESM2 and UKESM1 are similar with both having ERFari = -0.48 Wm^{-2} wirh SARFs of -0.69 Wm^{-2} (MRI-ESM2) and -0.74 Wm^{-2} (UKESM1). The OC results have the SARF much larger than the ERFari for CNRM-ESM2 (ERFari = -0.07 Wm^{-2}, SARF = -0.19 Wm^{-2}), NorESM2 (ERFari = -0.07 Wm^{-2}, SARF = -0.14 Wm^{-2}), but UKESM1 has similar values for both (ERFari = -0.15 Wm^{-2}, SARF = -0.13 Wm^{-2}).

Comparing the ERFaci values with those for the cloud adjustments (Section 3.2.1) for the BC experiments we have a similar value for the ERFaci and the cloud adjustments, although NorESM2 has a higher ERFaci than both the other models, which is double the cloud adjustments for this model. For the SO2 experiments the values of ERFaci and the overall cloud adjustments are in broad agreement, although the ERFaci tends to be larger and for the OC experiments the cloud adjustments tend to be about half the ERFaci values.

https://doi.org/10.5194/acp-2019-1205
Preprint. Discussion started: 13 March 2020

4.1.3 Intermodel Variability

A summary chart of the ERFs is shown in Fig 4 for those models with available results – it should be noted that not all models ran all the experiments. A table of the values for each model are in Table S2 in the supplemental materials.

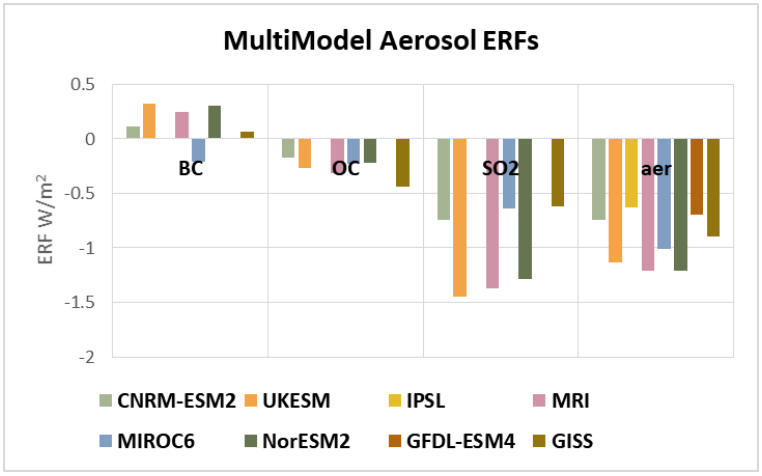

Fig. 3 Aerosol ERFs for the models with the available diagnostics for the aerosol species experiments.

For the piClim-BC results, the range of values is from -0.21 Wm^{-2} to 0.32 Wm^{-2}, where the MIROC6 model has a negative ERF for BC, contrasting with the positive values from the other models, as discussed in Section 3.2.1.

The experiments for the OC (organic carbon) have a range from -0.17 Wm^{-2} to -0.44 Wm^{-2}, and the variability between the models is much less than for the other experiments. The calculated ERFs for the SO2 experiment show a variation from -0.637 Wm^{-2} to -1.367 Wm^{-2}, with CNRM-ESM2-1, MIROC6 and GISS at the lower end of the range. These models show a smaller rapid adjustment to clouds, with GISS actually showing a slight positive cloud rapid adjustment (see fig S1); also note that CNRM-ESM2-1 does not include aerosol effects apart from the cloud-albedo effect.

The piClim-aer experiment which uses the 2014 values of aerosol precursors and PI (pre-industrial) values for CH4, N2O and ozone precursors shows a range from -0.633 Wm^{-2} to -1.2 Wm^{-2} among the models, making it difficult to narrow the range of uncertainty of aerosols from global models. However, the range in the CMIP6 models is consistent with that reported in Bellouin et al. (2019), who suggest a probable range of -1.60 to -0.65 W m^{-2} for the overall aerosol ERF. The multi-model means are shown in Table 4, with the standard deviation and the number of models used to calculate the means.

Table 4 Multimodel means for the ERFs based on the 30 year fixed SST timeslice experiments from the available model output.

https://doi.org/10.5194/acp-2019-1205
Preprint. Discussion started: 13 March 2020

	MultiModel Mean ERF (Wm^{-2})	Std Dev	Num Models
BC	0.14	0.18	6
OC	-0.27	0.09	6
SO2	-1.02	0.35	6
aer	-0.94	0.22	8

4.1.4 AOD and Burden

In order to break down the contributions of the various aerosol species to the overall ERF, we use the AOD (aerosol optical depth) for each of the species to scale their contributions to the overall aerosol ERF.

By looking at the single species piClim-BC, piClim-OC and piClim-SO2 experiments we can find the ERF due to the change in emission of these species from the PI control run, and the change in AOD resulting from this change, to arrive at a scale for the ERF as a function of the AOD change. Table 5 shows the scaling factors for the piClim-BC, piClim-SO2 and piClim-OC experiments for each of the three models which had the relevant optical depth diagnostics available.

Table 5 Values of ERF, ΔAOD and ERF/AOD change for aerosol experiments for CNRM-ESM2-, MIROC6, Nor-ESM2, models

BC Exp	**BC ERF**	**Change in BC AOD**	**ERF/AOD**
CNRM-ESM2	0.1140	0.0015	77.644
MIROC6	-0.2140	0.0006	-339.383
NorESM2	0.3000	0.0019	159.747
GISS	0.0647	0.002	31.648
MRI-ESM2	0.249	0.0073	34.22
OC Exp	**OC ERF**	**Change in OA AOD**	**ERF/AOD**
CNRM-ESM2	-0.1690	0.0030	-57.202
MIROC6	-0.2270	0.0065	-35.051
NorESM2	-0.2150	0.0053	-40.574
GISS	-0.4377	0.0041	-107.1627
MRI-ESM2	-0.32	0.0034	-94.389
SO2 Exp	**SO2 ERF**	**Change in SO4 AOD**	**ERF/AOD**

https://doi.org/10.5194/acp-2019-1205
Preprint. Discussion started: 13 March 2020

CNRM-ESM2	-0.7460	0.0118	-63.2203
MIROC6	-0.6370	0.0152	-41.9079
NorESM2	-1.2810	0.0099	-129.2389
GISS	-0.6217	0.0308	-20.2151
MRI-ESM2	-1.37	0.0279	-49.075

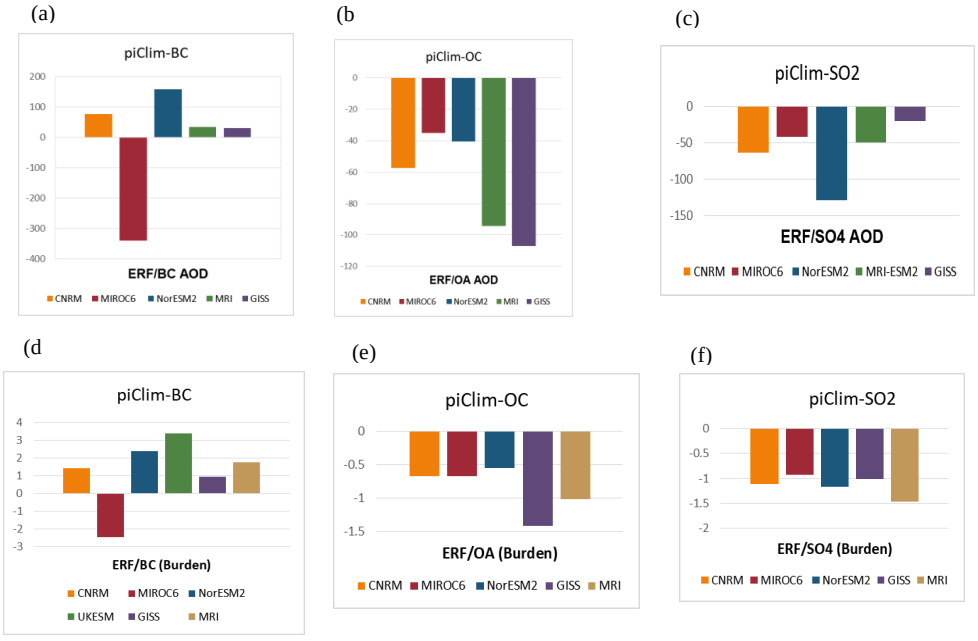

Fig. 4 ERF scaled against AOD and burdens (a) ERF/BC AOD in piClim-BC experiment, (b) ERF/OA AOD in piClim-OC experiment, (c) ERF/SO4 AOD in piClim-SO2 experiment. (d) ERF/burden for BC burden in piClim-BC experiment, (e) ERF/OA burden in piClim-OC experiment, (f) ERF/SO4 burden in piClim-SO2 experiment

The MIROC6 model results in a negative scaling for BC due to the negative ERF for this experiment for this model (Takemura & Suzuki 2019; Suzuki & Takemura 2019) (see Section 3.2.). The change in the BC OD is similar for CNRM-ESM2 and Nor-ESM2, and the scale factors reflect the differences in the ERF. The scaling for the SO4 in the NorESM2 experiment is twice that of the other models, suggesting a larger impact of the SO4 AOD on the ERF in this model. These values differ somewhat from those found in Myhre et al. (2013b) where they examined the radiative forcing normalised to the AOD using models in the AeroCom Phase II experiments. They found values for sulfate ranging from -8 Wm^{-2} to -21 Wm^{-2}, much lower than those in our results. However, it is important to note that in the Aerocom Phase II experiments the cloud and cloud optical properties are identical between their control and perturbed runs, so no aerosol indirect effects are included. For the BC experiment their values range from 84 Wm^{-2} to 216 Wm^{-2}, broadly similar to the results presented here (with the exception of the anomalous MIROC6 result); this may suggest that the cloud indirect effects are less important here. Their results for OA (organic aerosols) which include fossil fuel and biofuel emissions have values ranging from -10 Wm^{-2} to

https://doi.org/10.5194/acp-2019-1205
Preprint. Discussion started: 13 March 2020

-26 Wm^{-2}, lower than our values for the piClim-OC experiments which range from -35 Wm^{-2} to -107 Wm^{-2} but include the cloud indirect effects here.

Using this scaling factor to convert the change in AOD to a change in ERF we can ascertain the contributions of the individual species to the overall ERF in the piClim-aer experiment, where the various aerosols were combined. The sum of the individual AODs from BC, SO4, OA, dust and sea salt combine to give the total aerosol AOD in this experiment. In Fig. 6 the relative contributions to the ERF from black carbon (BC), organic aerosols (OA)

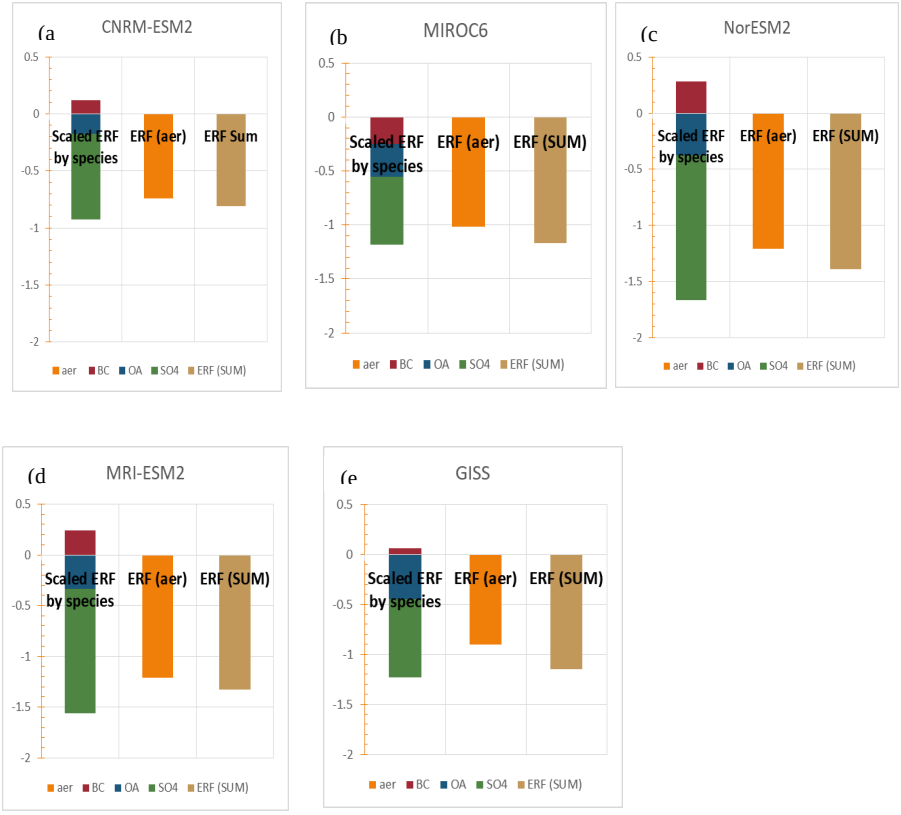

Fig. 5 The contributions to the ERF for piClim-aer from the individual species, compared with the ERF calculated directly from the piClim-aer experiment, and the sum of the scaled ERFs, for five of the models.

and sulfate (SO4) are shown for three of the models. The sum of the ERFS from the individual species is also compared to the ERF calculated from the piClim-aer experiment (NB the sea salt and dust contributions to the ERF are less than 1%, and not shown in this figure for clarity - the ERF/AOD scaling for these is presented in (Thornhill et al., 2020). There is considerable variation in the ERF for the piClim-aer experiments between models (see Section 3.2.1), but from this analysis the SO4 is the largest contributor in all cases, although in the case of the MIROC6 model its relative importance is reduced. The positive ERF contribution from the BC tends to offset that from the OA and SO4, except in the MIROC6 model, where the BC has a negative contribution to the ERF.

https://doi.org/10.5194/acp-2019-1205
Preprint. Discussion started: 13 March 2020

The difference between the calculated ERF from the sum of the scaled ERFs suggests that not all effects on the ERF are accounted for here, for example if the impact on clouds is different between the single-species experiments and the combined piClim-aer experiment we may be seeing a discrepancy due to cloud effects. As we assume that the change in ERF in the single species experiment is directly related to the change in AOD of that species in order to calculate the scaling, we investigated whether small changes in other species might also contribute to the ERF. We found that the changes in the other species were negligible in terms of their contribution to the ERF, so that the scaling derived from these experiments is reasonable (see figures in the Supplemental material).

Using the burden as a scaling factor following the same analysis as described for the AOD (fig 5) results in a largely similar result for the scaling factor, although interestingly the burden scaling for SO2 in the Nor-ESM2 model is similar to the other models.

4.2 Reactive gases

The different Earth system models include different degrees of complexity in their chemistry, so their responses to changes in reactive gas concentrations or emissions differ. NorESM2 has no atmospheric chemistry, so there is no change to ozone (tropospheric or stratosphere) or to aerosol oxidation following changes in methane or N_2O concentrations. CNRM-ESM2 includes stratospheric ozone chemistry and no changes to aerosol oxidation. UKESM1, GFDL-ESM4, CESM2-WACCM, BCC-ESM1, GISS-E2 and MRI-ESM2 all include tropospheric and stratospheric ozone chemistry as well as changes to aerosol oxidation rates. The ERFs calculated for the reactive gases for several models are shown in Fig. 6, with the multimodel means given in Table 6.
The contributions from gas-phase and aerosol changes to the ERF can be pulled apart to some extent by using the clear-sky and aerosol-free radiation diagnostics (Table 7). The direct aerosol forcing (ERFari) is diagnosed as for the aerosol experiments (section 3.1.3). For gas-phase experiments the diagnosed cloud interactions (ERFaf-ERFcsaf) comprise the ERFaci from effects on aerosol chemistry (as in section 3.1.3) but also any cloud adjustments to the gas-phase species, and effects of cloud masking on the gas-phase forcing. The clear-sky aerosol-free diagnostic (ERFcsaf) is an indication of the gas-phase forcing (ignoring cloud masking effects).

https://doi.org/10.5194/acp-2019-1205
Preprint. Discussion started: 13 March 2020

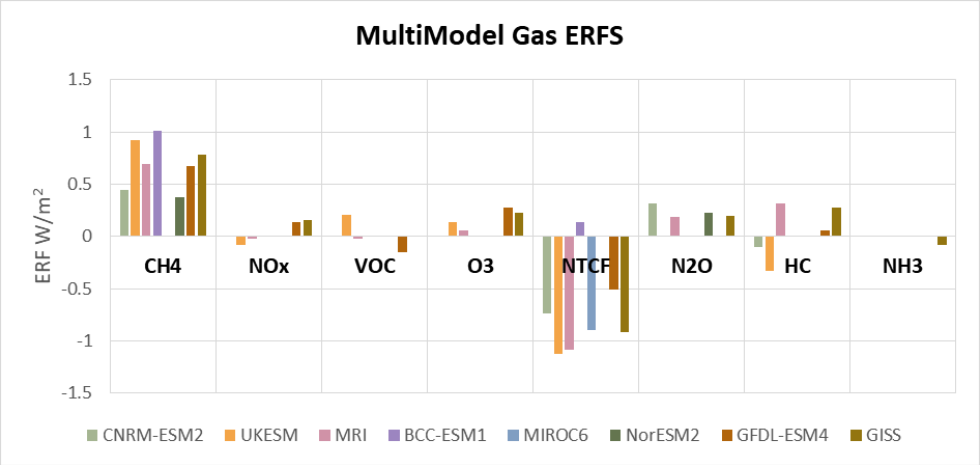

Fig. 6 Multimodel comparison for the ERFs for the chemically reactive species.

Table 6 Multi model means for the ERFs for chemically reactive species

	MultiModel Mean (Wm^{-2})	**Std Dev**	**Num Models**
CH4	0.70	0.22	7
Nox	0.05	0.10	4
VOC	0.06	0.16	4
O3	0.17	0.08	4
NTCF	-0.73	0.40	7
N2O	0.23	0.05	4
HC	0.04	0.24	5

4.2.1 ERF vs SARF

For methane the ERFs are largest for those models that include tropospheric ozone chemistry reflecting the increased forcing from ozone production. The tropospheric adjustments are negative for all models except UKESM1 (Fig 7). The negative cloud adjustment comes from an increase in the LW emissions, possibly due to less high cloud. In UKESM1 O'Connor et al (Submitted a) show that methane decreases sulfate new particle formation, thus reducing cloud albedo and hence a positive cloud adjustment in that model.

For N_2O results are available for models CNRM-ESM2, NorESM2, MRI-ESM2, and GISS-E2. NorESM2 does not include any ozone depletion from N_2O, although the ERF and SARF are higher than for CNRM-ESM2. There appears little net rapid adjustment to N_2O. Note that due to the method of calculating the all-sky IRF (section 3.1.2), the IRF and the adjustment terms do not sum to give the ERF.

https://doi.org/10.5194/acp-2019-1205
Preprint. Discussion started: 13 March 2020

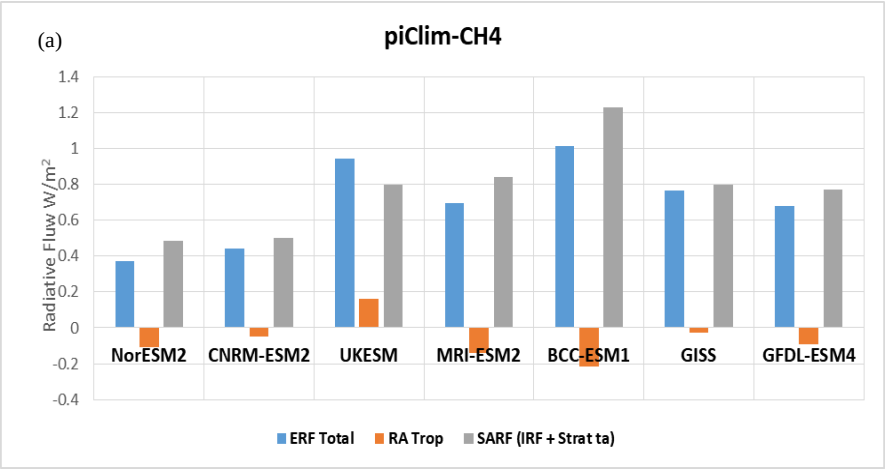

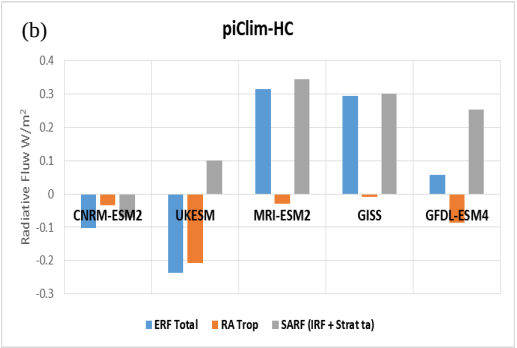

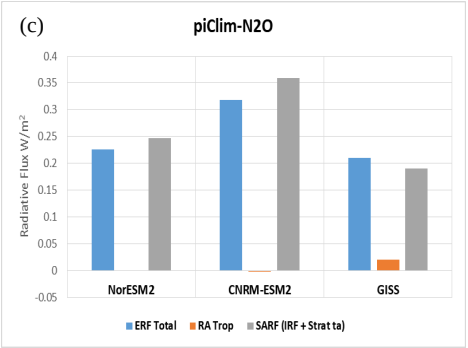

Fig. 7 Breakdown of the ERF into SARF and tropospheric rapid adjustments for the chemically reactive species (a) for piClim-CH4 experiments, (b) for piClim-HC experiments, (c) for piClim-N2O experiments.

The models respond very differently to changes in halocarbons. For CNRM-ESM2, UKESM1 and GFDL-ESM4 the ERFs are negative or only slightly positive (see also Morgenstern et al. submitted), whereas for GISS-E2 and MRI-ESM2 the ERFs and SARF are both strongly positive. The differences in stratospheric ozone destruction in these models is not sufficient to explain the intermodel differences.

Table 7 Calculations of ERFari, ERFaci (cloud) and ERFcs,af for the chemically reactive species

	UKESM			GFDL-ESM4			CNRM-ESM2			NorESM2			MRI-ESM2		
	ERFari	csaf	cloud	ERFari	csaf	cloud	ERFari	csaf	cloud	ERFari	csaf	cloud	ERFari	csaf	cloud
CH4	0.01	0.84	0.08	-0.01	0.91	-0.22	0.00	0.56	-0.12	-0.01	0.48	-0.10	0.00	0.91	-0.21
HC	-0.01	-0.05	-0.27	-0.02	0.22	-0.14	-0.01	-0.02	-0.08				-0.02	0.50	-0.17
N2O							0.00	0.41	-0.09	-0.01	0.24	-0.00	0.00	0.23	-0.03
O3	-0.02	0.17	-0.01	-0.04	0.49	-0.18							0.00	0.24	-0.18
NOx	-0.02	0.07	-0.13	-0.02	0.25	-0.09							-0.01	0.03	-0.04
VOC	0.00	0.09	0.12	-0.12	0.17	-0.20							0.00	0.17	-0.35

https://doi.org/10.5194/acp-2019-1205
Preprint. Discussion started: 13 March 2020

4.2.2 Ozone changes

To understand the contribution of ozone to the diagnosed ERFs, the column changes are diagnosed (figure 8). Increased CH_4 concentrations increases both tropospheric and stratospheric ozone by 2.6±0.3 and 3.3±1.2 Dobson Units respectively. Scaling these by the assumed radiative efficiency give a SARF for ozone produced by methane of 0.25±0.05 W m^{-2}. Results are similar across all the models that include tropospheric chemistry. VOC emissions increase tropospheric ozone. For GFDL-ESM4 and MRI-ESM2 stratospheric ozone increases too, however it decreases in GISS-E2. The impact of NO_X emissions is predominantly on tropospheric ozone, although MRI-ESM2 also has a large stratospheric response to NO_X (and also to O3 and NTCF) . The O3 experiment comprised both NOx and VOC emission changes. The tropospheric ozone column in this experiment is slightly larger than the sum of the NOx and VOC experiments due to non-linearities in the chemistry (Stevenson et al. 2013). The ozone changes when aerosol emissions are included too (NTCF) is slightly smaller than in O3, showing that these aerosols act to slightly depress the tropospheric ozone.

There is a larger variation across models in the stratospheric ozone depletion from halocarbons -38.8 DU in UKESM1 to -10.6 DU in CESM2-WACCM.

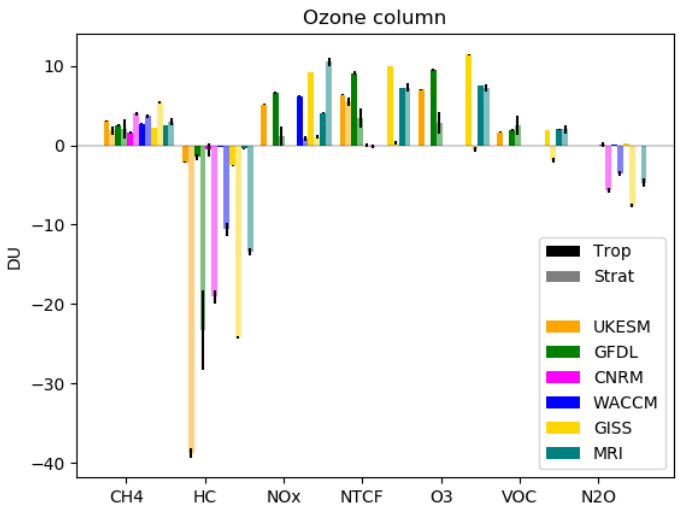

Fig. 8 Changes in column in Dobson Units (DU) of tropospheric (dark bars) and stratospheric ozone (light bars) for each experiment. Error bars show error on the mean due to interannual variability in each model.

4.2.3 Comparison with greenhouse gas forcings

The ERFs diagnosed for the gas-phase changes are compared with the expected radiative forcings in figure 9. The SARF from the well-mixed gases are given by Etminan et al. (2016) for CH_4 and N_2O, and by WMO (2018) for

https://doi.org/10.5194/acp-2019-1205
Preprint. Discussion started: 13 March 2020

the halocarbons (the halocarbon changes are slightly different in each model). The SARF for tropospheric ozone is estimated to be 0.042±0.005 W m^{-2} DU^{-1} (Stevenson et al. 2013). The SARF for stratospheric ozone is strongly dependent on its altitude. For the CH_4, NO_X and VOC experiments we assume that stratospheric ozone changes are close to the tropopause and the tropospheric ozone SARF can be used. For the N_2O and HC experiment we do not have a means to estimate the SARF from ozone changes.

For methane the ERFs are all lower than the expected GHG SARF (except for UKESM1) which is likely due to the negative cloud adjustments (although BCC-ESM1 included ozone chemistry the column ozone changes were not provided). The diagnosed ERFcsaf and SARF agree better with the expected SARF though it is notable that in NorESM2 and CNRM-ESM2 these are still lower than expected. For N_2O the modelled radiative forcing (of all kinds) is larger than expected for NorESM2, CNRM-ESM2 and CESM-WACCM. For UKESM1 the modelled N_2O ERF is lower than the expected SARF due to increased aerosol forcing (O'Connor et al. submitted b), whereas the ERFcsaf is slightly higher. For halocarbons the estimate for GFDL agrees quite well with the modelled SARF. The SARF for CNRM-ESM2 and ERFcsaf for UKESM1 is less than expected, partly due to stratospheric ozone depletion which is not accounted for here. The modelled ERF for UKESM1 is strongly negative due to increased aerosols ((O'Connor1 F. M., 2019) submitted, Morgenstern et al. submitted). The estimated ozone SARF from the NO_X, VOC and O_3 experiments agrees with the ERFcsaf for GFDL, but it strongly overestimates the ERFcsaf for MRI-ESM2. MRI-ESM2 has a very strong stratospheric ozone response to NOx and it is likely that using the tropospheric ozone radiative efficiency to scale this is inappropriate.

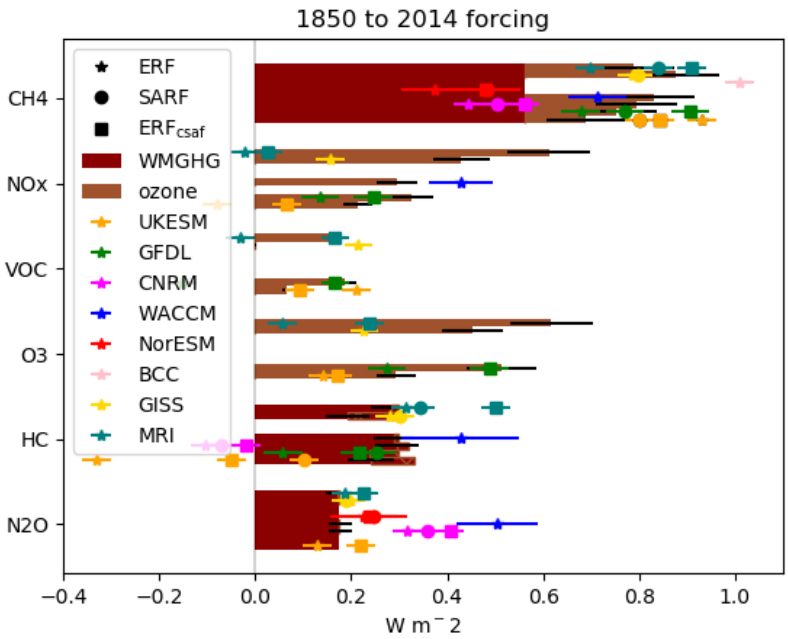

Fig. 9 Estimated SARF from the greenhouse gas changes (WMGHGs and ozone) using Etminan et al. 2016 for the WMGHG radiative efficiencies. Hatched bars show decreases in tropospheric ozone (not stratospheric). Symbols show the modelled ERF, SARF and ERFcsaf (estimate of gas-phase clear-sky ERF) – see key. Uncertainties on the bars are due to uncertainties in radiative efficiencies. Uncertainties on the symbols are errors in the mean due to interannual variability in the model diagnostic.

https://doi.org/10.5194/acp-2019-1205
Preprint. Discussion started: 13 March 2020

4.2.4 Methane Lifetime

In the CMIP6 setup the modelled methane concentrations do not respond to changes in oxidation rates. The methane lifetime is diagnosed (which includes stratospheric loss as parameterised within each model) and assuming a loss to soil with a lifetime of 120 years (Myhre et al., 2013b) and this can be used to infer the methane changes that would be expected if methane were allowed to vary. Figure 10 shows the methane lifetime response is large and negative for NO_x emissions, with a smaller positive change for VOC emissions. Halocarbon concentration increases decrease the methane lifetime, as ozone depletions leads to increased UV in the troposphere and increased methane loss to chlorine in the stratosphere (Stevenson et al. submitted). The lifetime response to changing methane concentrations can be used to diagnose the methane lifetime feedback factor *f* (Fiore et al. 2009). The results here give *f*=1.32, 1.30, 1.41, 1.33, 1.25, 1.31 (mean 1.32±0.05) for UKESM1, GFDL-ESM4, BCC-ESM1, CESM-WACCM. This is in very good agreement with AR5.

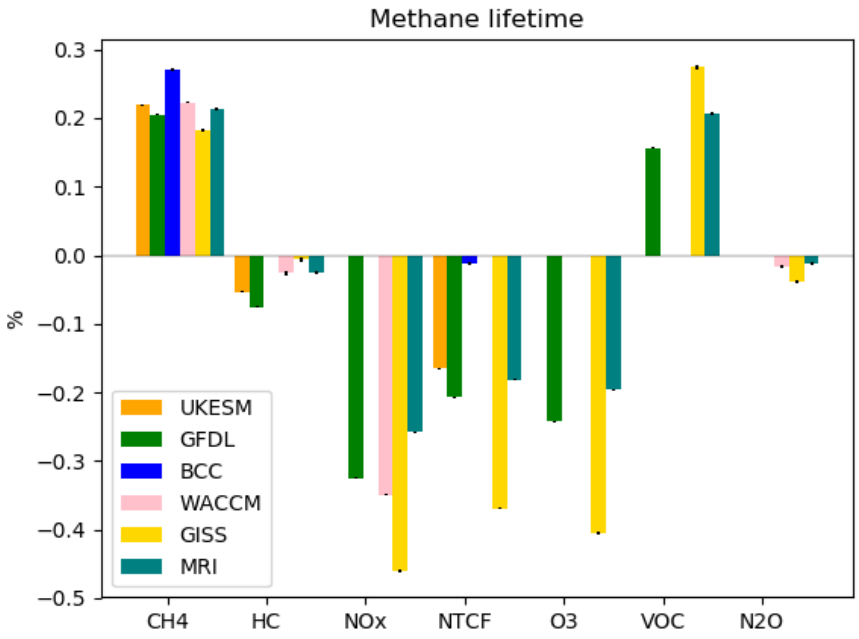

Fig. 10 Changes in methane lifetime (%), for each experiment. Uncertainties are errors on the mean from interannual variability.

4.2.5 Total ERFs

The methane lifetime changes can be converted to expected changes in concentration if methane were allowed to freely evolve following Fiore et al. (2009), using the *f*-factors appropriate to each model (section 3.3.4). The inferred radiative forcing is based on radiative efficiency of methane (Etminan et al. 2016). The methane changes

https://doi.org/10.5194/acp-2019-1205
Preprint. Discussion started: 13 March 2020

also have implications for ozone production, so we assume an ozone SARF per ppb of CH_4 diagnosed for each model from section 3.3.3.

The breakdown of the information from the analyses above is shown in Fig. 11, using the SARF calculated for the gases (WMGHGs and ozone), the changes in methane lifetime and the ERFari and cloud contributions for the aerosols for models where this is available. The contributions from methane lifetime changes have also been added to the diagnosed ERF as these aren't accounted for in the models. Differences between the diagnosed ERF (stars) and the sum of the components (crosses) then shows to what extent this decomposition into components can account for the modelled ERF. For many of the species, this breakdown is reasonable, and illustrates that cloud radiative effects make significant contributions to the total radiative impacts of WMGHGs and ozone precursors. This analysis cannot distinguish between cloud effects due to changes in atmospheric temperature profiles or those due to increased cloud nucleation from aerosols Differences between "sum" and ERF are largest for N_2O and halocarbons. For the halocarbons the "sum" is typically larger than the ERFs, since the radiative impact of stratospheric ozone depletion is ignored in the "sum". For N_2O the "sum" is typically smaller than the RFs, so this difference would become even larger when including any ozone depletion.

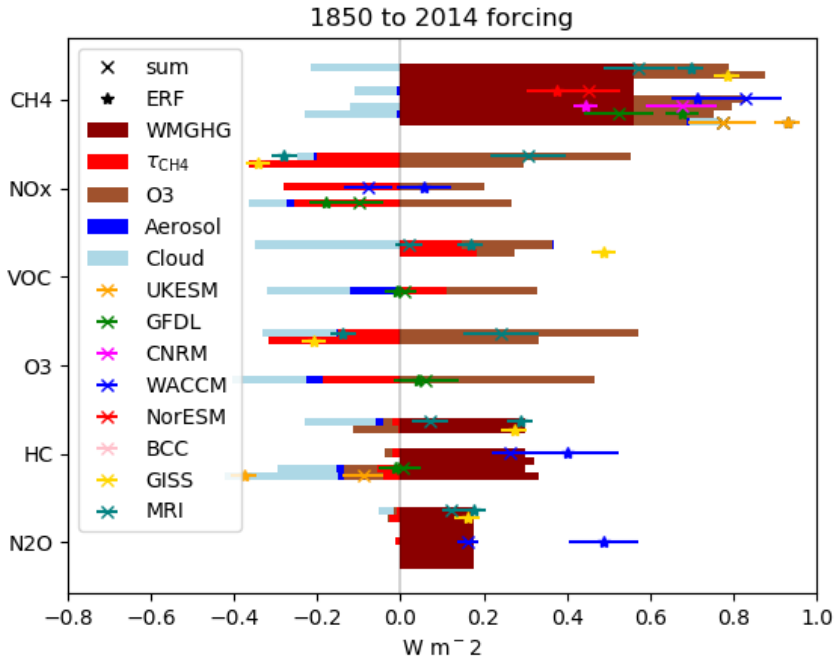

Fig. 11 SARF for WMGHGs, ozone and diagnosed changes in methane. Model diagnosed direct aerosol RF and cloud radiative effect. Crosses mark the sum of the five terms for each model. Stars mark the diagnosed ERF with the effect of methane lifetime (on methane and ozone) added. Differences between stars and crosses shows undiagnosed contributions. Uncertainties on the sum are mainly due to the uncertainties in the radiative efficiencies. Uncertainties in the ERF are errors on the mean due to interannual variability. Note for WACCM, BCC, GISS the breakdown into aerosol and cloud effects is unavailable.

https://doi.org/10.5194/acp-2019-1205
Preprint. Discussion started: 13 March 2020

5. Discussion

For all of the species shown we see considerable variation in the calculated ERFs across the models, which is due in part to differences in the model aerosol and chemistry schemes; not all models have interactive schemes for all of the species, and whether or not chemistry is considered will impact the evolution of some of the aerosol species. We can use the differences in model complexity from the multimodel approach together with the separation of the effects of the various species in the individual AerChemMIP experiments to understand how the various components contribute to the overall ERFs we have calculated.

5.1 Aerosols

The 1850-2014 mean ERFs for SO2, OC and BC are: -0.94 +/- 0.15 Wm^{-2} for SO2, -0.27 +/- 0.04 Wm^{-2} for OC, and 0.14 +/- 0.08 Wm^{-2} for BC. The total ERF for the aerosols is -0.94 +/- 0.08 Wm^{-2}, within the range of -1.65 to 0.6 Wm^{-2} reported by (Bellouin et al., 2019).

The radiative kernels and double call diagnostics are used to separate the direct and cloud effects of aerosols for those models where all the relevant diagnostics are available. These two methods broadly agree on the cloud contribution for the BC, SO2 and OC experiments, although we find a smaller cloud adjustment to black carbon compared to other studies (Samset and Myhre, 2015;Stjern et al., 2017;Smith et al., 2018).

As the CLISCCP cloud diagnostics become available for more of the CMIP6 models, it will be possible to do a direct calculation of the cloud rapid adjustments using the kernels from (Zelinka et al., 2014) and compare those with the adjustments calculated using the kernel difference method described in (Smith et al., 2018) and used here (Section 3.1.2).

The values diagnosed for the ERFari (for the models we have available diagnostics for) in CMIP6 are similar to those from CMIP5 (Myhre et al., 2013a) where they reported values for sulfate of -0.4 (-0.6 to –0.2) Wm^{-2} compared to our -0.36 (-0.19 to -0.48) Wm^{-2} for the SO2 experiment, for OC they found -0.09 (-0.16 to –0.03) Wm^{-2} compared to our value of -0.09 (-0.07 to -0.15) Wm^{-2} and for BC they had +0.4 (+0.05 to +0.80) compared to our value of 0.28 (0.13- 0.38) Wm^{-2}, so broadly the ERFari for the individual species agree with those found in the previous set of models used in CMIP5. The overall aerosol ERFari from AR5 is reported as in the range -1.5 to 0.4 Wm^{-2}, compared to values reported here in the range -0.16 to 0.03 Wm^{-2}.

The radiative efficiencies per AOD calculated here are generally larger than those from the AeroCom Phase II experiments (Myhre et al., 2013b), with the caveat that the models included here did not have fixed clouds, so that indirect effects would be included; the BC efficiencies are however closer to those in AeroCom Phase II, perhaps indicative of a lesser effect of the cloud effects in the case of BC. The radiative efficiencies per AOD calculated here are generally larger than those from the AeroCom Phase II experiments (Myhre et al., 2013b), with the caveat that the models included here did not have fixed clouds, so that indirect effects would be included; the BC efficiencies are however closer to those in AeroCom Phase II, perhaps indicative of a lesser effect of the cloud effects in the case of BC.

5.2 Reactive gases

https://doi.org/10.5194/acp-2019-1205
Preprint. Discussion started: 13 March 2020

The diagnosed ERFs from methane, N_2O, halocarbons and ozone precursors are: 0.80±0.13, 0.26±0.15, 0.15±0.27 and 0.17±0.08 W m^{-2} (excluding CNRM-ESM2 and NorESM2 as these do not have tropospheric ozone chemistry) . These compare with 0.79±0.13, 0.17±0.03, 0.18±0.15 and 0.22±0.14 W m^{-2} from AR5 (Myhre et al., 2013a) - where the effects on methane lifetime and CO_2 have been removed from the AR5 calculations, and the halocarbons are for CFCs and HCFCs only. Section 3.3.5 show that cloud effects can make a significant contribution to the overall ERF even for WMGHGs. However, clouds cannot explain all the differences. The ERF for N_2O is larger than estimated in AR5. The multi-model ERF for halocarbons is similar to AR5, although the models have a wide spread with some showing significantly lower ERFs and some significantly higher. The difference in halocarbon ERF could be due to strong ozone depletion in these models.

The estimated ozone SARFs from the changes in levels of methane, NOx and VOC from 1850 to 2014 are 0.24±0.05, 0.32±0.05, and 0.17±0.06 W m^{-2} compared to 0.24±0.13, 0.14±0.09, and 0.11±0.05 W m^{-2} in CMIP5 (Myhre et al., 2013a). The NOx contribution stands out as being larger in this study. The CMIP5 results did not account for the radiative impact of ozone changes above the tropopause, but this is not enough to account for the difference in the NO_x-induced ozone compared to AR5.

The overall effect of NTCF emissions (excluding methane and other WMGHGs) on the 1850-2014 ERF experienced by models that include tropospheric chemistry is strongly negative (-0.70±0.47 W m^{-2}) due to the dominance of the aerosol forcing over that from ozone. There is a large spread in the NTCF forcing due to the different treatment of atmospheric chemistry within these models. Models without tropospheric and/or stratospheric chemistry prescribe varying ozone levels which are not included in the NTCF experiment. Hence the overall forcing experienced by these models due to ozone and aerosols will be different from that diagnosed here.

6. Conclusion

The experimental setup and diagnostics in CMIP6 have allowed us for the first time to calculate the effective radiative forcing (ERF) for present day reactive gas and aerosol concentrations and emissions in a range of Earth system models. Quantifying the forcing in these models is an essential step to understanding their climate responses.

This diagnoses also allows us to quantify the radiative responses to perturbations in individual species or groups of species. These responses include physical adjustments to the imposed forcing as well as chemical adjustments and adjustments related to the emissions of natural aerosols. The total adjustment is therefore a complex combination of individual process, but the diagnosed ERF implicitly includes these and represents the overall forcing experienced by the models.

We find that the ERF from well-mixed greenhouse gases (methane, nitrous oxide and halocarbons) is significantly different to the SARF estimated from standard formulae. This indicates that Earth system processes need to be taken into account when understanding the contribution WMGHGs have made to present climate and when projecting the climate effects of different WMGHG scenarios.

https://doi.org/10.5194/acp-2019-1205
Preprint. Discussion started: 13 March 2020

5. Acknowledgements

GT, WC, MM, FO'C, DO, MS, CS acknowledge funding received from the European Union's Horizon 2020 research and innovation programme under grant agreement No 641816 (CRESCENDO).

FMO'C, JPM were funded by the Met Office Hadley Centre Climate Programme funded by BEIS and Defra (GA01101). GZ was supported by the NZ government's Strategic Science Investment Fund (SSIF) through the NIWA programme CACV.

We acknowledge the World Climate Research Programme, which, through its Working Group on Coupled Modelling, coordinated and promoted CMIP6. We thank the climate modeling groups for producing and making available their model output, the Earth System Grid Federation (ESGF) for archiving the data and providing access, and the multiple funding agencies who support CMIP6 and ESGF.

6. Author Contributions

Manuscript preparation was done by GDT, WJC, RJK, DO and additional contributions from all co-authors. Model simulations were set up, reviewed and/or ran by DO, FMO'C, NLA, MD, LE, LH, J-FL, MMichou, MMills, JM, PN, VN, NO, MS, TT, ST, TW, GZ, JZ. Analysis was carried out by GT, WC, RK, DO.

7. Data Availability

All data from the various earth system models used in this paper are available on the Earth System Grid Federation Website, and can be downloaded from there. https://esgf-index1.ceda.ac.uk/search/cmip6-ceda/

8. References

Abdul-Razzak, H., and Ghan, S. J.: A parameterization of aerosol activation: 2. Multiple aerosol types, Journal of Geophysical Research: Atmospheres, 105, 6837-6844, 10.1029/1999jd901161, 2000.

Albrecht, B. A.: Aerosols, cloud microphysics, and fractional cloudiness, Science, 245, 1227-1230, 1989.

Archibald, A. T., O'Connor, F. M., Abraham, N. L., Archer-Nicholls, S., Chipperfield, M. P., Dalvi, M., Folberth, G. A., Dennison, F., Dhomse, S. S., Griffiths, P. T., Hardacre, C., Hewitt, A. J., Hill, R., Johnson, C. E., Keeble, J., Köhler, M. O., Morgenstern, O., Mulchay, J. P., Ordóñez, C., Pope, R. J., Rumbold, S., Russo, M. R., Savage, N., Sellar, A., Stringer, M., Turnock, S., Wild, O., and Zeng, G.: Description and evaluation of the UKCA stratosphere-troposphere chemistry scheme (StratTrop vn 1.0) implemented in UKESM1, Geosci. Model Dev. Discuss., 2019, 1-82, 10.5194/gmd-2019-246, 2019.

Bellouin, N., Quaas, J., Gryspeerdt, E., Kinne, S., Stier, P., Watson-Parris, D., Boucher, O., Carslaw, K. S., Christensen, M., Daniau, A.-L., Dufresne, J.-L., Feingold, G., Fiedler, S., Forster, P., Gettelman, A., Haywood, J. M., Lohmann, U., Malavelle, F., Mauritsen, T., McCoy, D. T., Myhre, G., Mülmenstädt, J., Neubauer, D., Possner, A., Rugenstein, M., Sato, Y., Schulz, M., Schwartz, S. E., Sourdeval, O., Storelvmo, T., Toll, V., Winker, D., and Stevens, B.: Bounding global aerosol radiative forcing of climate change, Reviews of Geophysics, n/a, 10.1029/2019rg000660, 2019.

Block, K., and Mauritsen, T.: Forcing and feedback in the MPI-ESM-LR coupled model under abruptly quadrupled CO2, Journal of Advances in Modeling Earth Systems, 5, 676-691, 10.1002/jame.20041, 2013.

Boucher, O. e. a.: Clouds and Aerosols, In: Climate Change 2013: The Physical Science Basis. Contribution of Working Group I to the Fifth Assessment Report of the Intergovernmental Panel on Climate Change, in, Cambridge University Press, Cambridge, United Kingdom and New York, NY, USA., 2013.

Chung, E.-S., and Soden, B. J.: An Assessment of Direct Radiative Forcing, Radiative Adjustments, and Radiative Feedbacks in Coupled Ocean–Atmosphere Models, Journal of Climate, 28, 4152-4170, 10.1175/jcli-d-14-00436.1, 2015.

Collins, W. J., Lamarque, J. F., Schulz, M., Boucher, O., Eyring, V., Hegglin, M. I., Maycock, A., Myhre, G., Prather, M., Shindell, D., and Smith, S. J.: AerChemMIP: quantifying the effects of chemistry and aerosols in CMIP6, Geosci. Model Dev., 10, 585-607, 10.5194/gmd-10-585-2017, 2017.

Deushi, M., and Shibata, K.: Development of a Meteorological Research Institute Chemistry-Climate Model version 2 for the Study of Tropospheric and Stratospheric Chemistry, Papers in Meteorology and Geophysics, 62, 1-46, 10.2467/mripapers.62.1, 2011.

Emmons, L. K., Walters, S., Hess, P. G., Lamarque, J. F., Pfister, G. G., Fillmore, D., Granier, C., Guenther, A., Kinnison, D., Laepple, T., Orlando, J., Tie, X., Tyndall, G., Wiedinmyer, C., Baughcum, S. L., and Kloster, S.: Description and evaluation of the Model for Ozone and Related chemical Tracers, version 4 (MOZART-4), Geosci. Model Dev., 3, 43-67, 10.5194/gmd-3-43-2010, 2010.

Eyring, V., Bony, S., Meehl, G. A., Senior, C. A., Stevens, B., Stouffer, R. J., and Taylor, K. E.: Overview of the Coupled Model Intercomparison Project Phase 6 (CMIP6) experimental design and organization, Geosci. Model Dev., 9, 1937-1958, 10.5194/gmd-9-1937-2016, 2016.

Forster, P. M., Richardson, T., Maycock, A. C., Smith, C. J., Samset, B. H., Myhre, G., Andrews, T., Pincus, R., and Schulz, M.: Recommendations for diagnosing effective radiative forcing from climate models for CMIP6, Journal of Geophysical Research: Atmospheres, 121, 12,460-412,475, doi:10.1002/2016JD025320, 2016.

Gettelman, A., Mills, M. J., Kinnison, D. E., Garcia, R. R., Smith, A. K., Marsh, D. R., Tilmes, S., Vitt, F., Bardeen, C. G., McInerny, J., Liu, H. L., Solomon, S. C., Polvani, L. M., Emmons, L. K., Lamarque, J. F., Richter, J. H., Glanville, A. S., Bacmeister, J. T., Phillips, A. S., Neale, R. B., Simpson, I. R., DuVivier, A. K., Hodzic, A., and Randel, W. J.: The Whole Atmosphere Community Climate Model Version 6 (WACCM6), Journal of Geophysical Research: Atmospheres, n/a, 10.1029/2019JD030943, 2019.

Ghan, S. J.: Technical Note: Estimating aerosol effects on cloud radiative forcing, Atmos. Chem. Phys., 13, 9971-9974, 10.5194/acp-13-9971-2013, 2013.

Hoesly, R. M., Smith, S. J., Feng, L., Klimont, Z., Janssens-Maenhout, G., Pitkanen, T., Seibert, J. J., Vu, L., Andres, R. J., Bolt, R. M., Bond, T. C., Dawidowski, L., Kholod, N., Kurokawa, J.-i., Li, M., Liu, L., Lu, Z., Moura, M. C. P., O'Rourke, P. R., and Zhang, Q.: Historical (1750–2014) anthropogenic emissions of reactive gases and aerosols from the Community Emissions Data System (CEDS), Geoscientific Model Development (Online), Medium: ED; Size: p. 369-408, 2018.

Horowitz, L. W., Walters, S., Mauzerall, D. L., Emmons, L. K., Rasch, P. J., Granier, C., Tie, X., Lamarque, J.-F., Schultz, M. G., Tyndall, G. S., Orlando, J. J., and Brasseur, G. P.: A global simulation of tropospheric ozone and related tracers: Description and evaluation of MOZART, version 2, Journal of Geophysical Research: Atmospheres, 108, 10.1029/2002jd002853, 2003.

Jones, A., Roberts, D. L., Woodage, M. J., and Johnson, C. E.: Indirect sulphate aerosol forcing in a climate model with an interactive sulphur cycle, Journal of Geophysical Research: Atmospheres, 106, 20293-20310, 10.1029/2000jd000089, 2001.

Kawai, H., Yukimoto, S., Koshiro, T., Oshima, N., Tanaka, T., Yoshimura, H., and Nagasawa, R.: Significant improvement of cloud representation in the global climate model MRI-ESM2, Geosci. Model Dev., 12, 2875-2897, 10.5194/gmd-12-2875-2019, 2019.

Khairoutdinov, M., and Kogan, Y.: A New Cloud Physics Parameterization in a Large-Eddy Simulation Model of Marine Stratocumulus, Monthly Weather Review, 128, 229-243, 10.1175/1520-0493(2000)128<0229:ancppi>2.0.co;2, 2000.

Kirkevåg, A., Grini, A., Olivié, D., Seland, Ø., Alterskjær, K., Hummel, M., Karset, I. H. H., Lewinschal, A., Liu, X., Makkonen, R., Bethke, I., Griesfeller, J., Schulz, M., and Iversen, T.: A production-tagged aerosol module for Earth system models, OsloAero5.3 – extensions and updates for CAM5.3-Oslo, Geosci. Model Dev., 11, 3945-3982, 10.5194/gmd-11-3945-2018, 2018.

Meinshausen, M., Vogel, E., Nauels, A., Lorbacher, K., Meinshausen, N., Etheridge, D. M., Fraser, P. J., Montzka, S. A., Rayner, P. J., Trudinger, C. M., Krummel, P. B., Beyerle, U., Canadell, J. G., Daniel, J. S., Enting, I. G., Law, R. M., Lunder, C. R., O'Doherty, S., Prinn, R. G., Reimann, S., Rubino, M., Velders, G. J. M., Vollmer, M. K., Wang, R. H. J., and Weiss, R.: Historical greenhouse gas concentrations for climate modelling (CMIP6), Geosci. Model Dev., 10, 2057-2116, 10.5194/gmd-10-2057-2017, 2017.

Mills, M. J., Schmidt, A., Easter, R., Solomon, S., Kinnison, D. E., Ghan, S. J., Neely Iii, R. R., Marsh, D. R., Conley, A., Bardeen, C. G., and Gettelman, A.: Global volcanic aerosol properties derived from emissions, 1990–2014, using CESM1(WACCM), Journal of Geophysical Research: Atmospheres, 121, 2332-2348, 10.1002/2015JD024290, 2016.

Morgenstern, O., Braesicke, P., O'Connor, F. M., Bushell, A. C., Johnson, C. E., Osprey, S. M., and Pyle, J. A.: Evaluation of the new UKCA climate-composition model – Part 1: The stratosphere, Geosci. Model Dev., 2, 43-57, 10.5194/gmd-2-43-2009, 2009.

Mulcahy, J. P., Jones, C., Sellar, A., Johnson, B., Boutle, I. A., Jones, A., Andrews, T., Rumbold, S. T., Mollard, J., Bellouin, N., Johnson, C. E., Williams, K. D., Grosvenor, D. P., and McCoy, D. T.: Improved Aerosol Processes and Effective Radiative Forcing in HadGEM3 and UKESM1, Journal of Advances in Modeling Earth Systems, 10, 2786-2805, 10.1029/2018ms001464, 2018.

Myhre, G., D. Shindell, F.-M. Bréon, W. Collins, J. Fuglestvedt, J. Huang, D. Koch, J.-F. Lamarque, D. Lee, B. Mendoza, T. Nakajima, A. Robock, G. Stephens, Takemura, T., and Zhang, H.: Anthropogenic and Natural Radiative Forcing. In: Climate Change 2013: The Physical Science Basis. Contribution of Working Group I to the Fifth Assessment Report of the Intergovernmental Panel on Climate Change, 2013a.

Myhre, G., Samset, B. H., Schulz, M., Balkanski, Y., Bauer, S., Berntsen, T. K., Bian, H., Bellouin, N., Chin, M., Diehl, T., Easter, R. C., Feichter, J., Ghan, S. J., Hauglustaine, D., Iversen, T., Kinne, S., Kirkevåg, A., Lamarque, J. F., Lin, G., Liu, X., Lund, M. T., Luo, G., Ma, X., van Noije, T., Penner, J. E., Rasch, P. J., Ruiz, A., Seland, Ø., Skeie, R. B., Stier, P., Takemura, T., Tsigaridis, K., Wang, P., Wang, Z., Xu, L., Yu, H., Yu, F., Yoon, J. H., Zhang, K., Zhang, H., and Zhou, C.: Radiative forcing of the direct aerosol effect from AeroCom Phase II simulations, Atmos. Chem. Phys., 13, 1853-1877, 10.5194/acp-13-1853-2013, 2013b.

O'Connor, F. M., Johnson, C. E., Morgenstern, O., Abraham, N. L., Braesicke, P., Dalvi, M., Folberth, G. A., Sanderson, M. G., Telford, P. J., Voulgarakis, A., Young, P. J., Zeng, G., Collins, W. J., and Pyle, J. A.: Evaluation of the new UKCA climate-composition model – Part 2: The Troposphere, Geosci. Model Dev., 7, 41-91, 10.5194/gmd-7-41-2014, 2014.

O'Connor1 F. M., N. L. A., 3, Mohit Dalvi1, Gerd Folberth1, Paul Griffiths2,3, Catherine Hardacre1, Ben T. Johnson1, Ron Kahana1, James Keeble2,3, Byeonghyeon Kim4, Olaf Morgenstern5, Jane P. Mulcahy1, Mark G. Richardson6, Eddy Robertson1, Jeongbyn Seo4, Sungbo Shim4, Joao C. Teixeira1, Steven Turnock1, Jonny Williams5, Andy Wiltshire1, and Guang Zeng5: Assessment of pre-industrial to present-day anthropogenic climate forcing in UKESM1, Atmospheric Chemistry and Physics, Submitted, 2019.

Pendergrass, A. G., Conley, A., and Vitt, F. M.: Surface and top-of-atmosphere radiative feedback kernels for CESM-CAM5, Earth Syst. Sci. Data, 10, 317-324, 10.5194/essd-10-317-2018, 2018.

Pincus, R., and Baker, M. B.: Effect of precipitation on the albedo susceptibility of clouds in the marine boundary layer, Nature, 372, 250-252, 10.1038/372250a0, 1994.

Samset, B. H., and Myhre, G.: Climate response to externally mixed black carbon as a function of altitude, Journal of Geophysical Research: Atmospheres, 120, 2913-2927, 10.1002/2014jd022849, 2015.

Samset, B. H., Myhre, G., Forster, P. M., Hodnebrog, Ø., Andrews, T., Faluvegi, G., Fläschner, D., Kasoar, M., Kharin, V., Kirkevåg, A., Lamarque, J.-F., Olivié, D., Richardson, T., Shindell, D., Shine, K. P., Takemura, T., and Voulgarakis, A.: Fast and slow precipitation responses to individual climate forcers: A PDRMIP multimodel study, Geophysical Research Letters, 43, 2782-2791, 10.1002/2016gl068064, 2016.

Sellar, A. A., Jones, C. G., Mulcahy, J., Tang, Y., Yool, A., Wiltshire, A., O'Connor, F. M., Stringer, M., Hill, R., Palmieri, J., Woodward, S., de Mora, L., Kuhlbrodt, T., Rumbold, S., Kelley, D. I., Ellis, R., Johnson, C. E., Walton, J., Abraham, N. L., Andrews, M. B., Andrews, T., Archibald, A. T., Berthou, S., Burke, E., Blockley, E., Carslaw, K., Dalvi, M., Edwards, J., Folberth, G. A., Gedney, N., Griffiths, P. T., Harper, A. B., Hendry, M. A., Hewitt, A. J., Johnson, B., Jones, A., Jones, C. D., Keeble, J., Liddicoat, S., Morgenstern, O., Parker, R. J., Predoi, V., Robertson, E., Siahaan, A., Smith, R. S., Swaminathan, R., Woodhouse, M. T., Zeng, G., and Zerroukat, M.: UKESM1: Description and evaluation of the UK Earth System Model, Journal of Advances in Modeling Earth Systems, n/a, 10.1029/2019ms001739, 2020.

Sherwood, S. C., Bony, S., Boucher, O., Bretherton, C., Forster, P. M., Gregory, J. M., and Stevens, B.: Adjustments in the Forcing-Feedback Framework for Understanding Climate Change, Bulletin of the American Meteorological Society, 96, 217-228, 10.1175/bams-d-13-00167.1, 2015.

Smith, C. J., Kramer, R. J., Myhre, G., Forster, P. M., Soden, B. J., Andrews, T., Boucher, O., Faluvegi, G., Fläschner, D., Hodnebrog, Ø., Kasoar, M., Kharin, V., Kirkevåg, A., Lamarque, J.-F., Mülmenstädt, J., Olivié, D., Richardson, T., Samset, B. H., Shindell, D., Stier, P., Takemura, T., Voulgarakis, A., and Watson-Parris, D.: Understanding Rapid Adjustments to Diverse Forcing Agents, Geophysical Research Letters, 45, 12,023-012,031, doi:10.1029/2018GL079826, 2018.

Soden, B. J., Held, I. M., Colman, R., Shell, K. M., Kiehl, J. T., and Shields, C. A.: Quantifying Climate Feedbacks Using Radiative Kernels, Journal of Climate, 21, 3504-3520, 10.1175/2007jcli2110.1, 2008.

Stjern, C. W., Samset, B. H., Myhre, G., Forster, P. M., Hodnebrog, Ø., Andrews, T., Boucher, O., Faluvegi, G., Iversen, T., Kasoar, M., Kharin, V., Kirkevåg, A., Lamarque, J.-F., Olivié, D., Richardson, T., Shawki, D., Shindell, D., Smith, C. J., Takemura, T., and Voulgarakis, A.: Rapid Adjustments Cause Weak Surface Temperature Response to Increased Black Carbon Concentrations, Journal of Geophysical Research: Atmospheres, 122, 11,462-411,481, 10.1002/2017jd027326, 2017.

Takemura, T., Nozawa, T., Emori, S., Nakajima, T. Y., and Nakajima, T.: Simulation of climate response to aerosol direct and indirect effects with aerosol transport-radiation model, Journal of Geophysical Research: Atmospheres, 110, 10.1029/2004jd005029, 2005.

Thornhill, G., Collins, W., Olivié, D., Archibald, A., Bauer, S., Checa-Garcia, R., Fiedler, S., Folberth, G., Gjermundsen, A., Horowitz, L., Lamarque, J. F., Michou, M., Mulcahy, J., Nabat, P., Naik, V., O'Connor, F. M., Paulot, F., Schulz, M., Scott, C. E., Seferian, R., Smith, C., Takemura, T., Tilmes, S., and Weber, J.: Climate-driven chemistry and aerosol feedbacks in CMIP6 Earth system models, Atmos. Chem. Phys. Discuss., 2020, 1-36, 10.5194/acp-2019-1207, 2020.

Tilmes, S., Hodzic, A., Emmons, L. K., Mills, M. J., Gettelman, A., Kinnison, D. E., Park, M., Lamarque, J. F., Vitt, F., Shrivastava, M., Campuzano-Jost, P., Jimenez, J. L., and Liu, X.: Climate Forcing and Trends of Organic Aerosols in the Community Earth System Model (CESM2), Journal of Advances in Modeling Earth Systems, n/a, 10.1029/2019MS001827, 2019.

Twomey, S.: Pollution and the planetary albedo, Atmospheric Environment (1967), 8, 1251-1256, https://doi.org/10.1016/0004-6981(74)90004-3, 1974.

van Marle, M. J. E., Kloster, S., Magi, B. I., Marlon, J. R., Daniau, A. L., Field, R. D., Arneth, A., Forrest, M., Hantson, S., Kehrwald, N. M., Knorr, W., Lasslop, G., Li, F., Mangeon, S., Yue, C., Kaiser, J. W., and van der Werf, G. R.: Historic global biomass burning emissions for CMIP6 (BB4CMIP) based on merging satellite observations with proxies and fire models (1750–2015), Geosci. Model Dev., 10, 3329-3357, 10.5194/gmd-10-3329-2017, 2017.

Watanabe, M., Suzuki, T., O'ishi, R., Komuro, Y., Watanabe, S., Emori, S., Takemura, T., Chikira, M., Ogura, T., Sekiguchi, M., Takata, K., Yamazaki, D., Yokohata, T., Nozawa, T., Hasumi, H., Tatebe, H., and Kimoto, M.:

https://doi.org/10.5194/acp-2019-1205
Preprint. Discussion started: 13 March 2020

Improved Climate Simulation by MIROC5: Mean States, Variability, and Climate Sensitivity, Journal of Climate, 23, 6312-6335, 10.1175/2010jcli3679.1, 2010.

Woodward, S.: Modeling the atmospheric life cycle and radiative impact of mineral dust in the Hadley Centre climate model, Journal of Geophysical Research: Atmospheres, 106, 18155-18166, 10.1029/2000jd900795, 2001.

Wu, T., Lu, Y., Fang, Y., Xin, X., Li, L., Li, W., Jie, W., Zhang, J., Liu, Y., Zhang, L., Zhang, F., Zhang, Y., Wu, F., Li, J., Chu, M., Wang, Z., Shi, X., Liu, X., Wei, M., Huang, A., Zhang, Y., and Liu, X.: The Beijing Climate Center Climate System Model (BCC-CSM): the main progress from CMIP5 to CMIP6, Geosci. Model Dev., 12, 1573-1600, 10.5194/gmd-12-1573-2019, 2019a.

Wu, T., Zhang, F., Zhang, J., Jie, W., Zhang, Y., Wu, F., Li, L., Liu, X., Lu, X., Zhang, L., Wang, J., and Hu, A.: Beijing Climate Center Earth System Model version 1 (BCC-ESM1): Model Description and Evaluation, Geosci. Model Dev. Discuss., 2019, 1-47, 10.5194/gmd-2019-172, 2019b.

Yukimoto, S., Kawai, H., Koshiro, T., Oshima, N., Yoshida, K., Urakawa, S., Tsujino, H., Deushi, M., Tanaka, T., Hosaka, M., Yabu, S., Yoshimura, H., Shindo, E., Mizuta, R., Obata, A., Adachi, Y., and Ishii, M.: The Meteorological Research Institute Earth System Model Version 2.0, MRI-ESM2.0: Description and Basic Evaluation of the Physical Component, 97, 931-965, 10.2151/jmsj.2019-051, 2019.

Zelinka, M. D., Andrews, T., Forster, P. M., and Taylor, K. E.: Quantifying components of aerosol-cloud-radiation interactions in climate models, Journal of Geophysical Research: Atmospheres, 119, 7599-7615, 10.1002/2014jd021710, 2014.